Supplementary Information for

Ambient Stability and Surface Adhesion of 2D Polyaramid Nano-Films

Michelle Quien *et al.*

Corresponding Author: Michael S. Strano, strano@mit.edu

The PDF file includes:

Mathematical Approximations to Gas-filled Bulges

Herein, we discuss different approximations of gas-filled bulges. Hencky's solution approximates the bulge as a uniform-thickness, circular isotropic membrane clamped at its boundaries without pre-tension and subjected to uniform lateral loading, and is the following expression:[1]

$$\Delta p = \frac{16EdK(\nu)}{a^4}\delta^3 \qquad \text{Equation S1}$$

where $K(\nu)$ is an infinite series dependent on the Poisson's ratio, ν, and thus Hencky's solution can be written as the following infinite summation:[2]

$$\frac{\delta}{d/2}(\mathrm{r}) = \left(\frac{\Delta p}{2E}\right)^{\frac{1}{3}}\left[a_0\left(1-\left(\frac{r}{d/2}\right)^2\right)+a_2\left(1-\left(\frac{r}{d/2}\right)^4\right)+a_4\left(1-\left(\frac{r}{d/2}\right)^6\right)+a_6\left(1-\left(\frac{r}{d/2}\right)^8\right)+\cdots\right]$$

Equation S2

where a_0 is a prefactor term dependent on the Poisson's ratio, ν.

We show in *Figure S1* the comparison of Hencky's solution, a 2nd order polynomial, and the 1-point model with AFM data of an experimental bulge, all of which have the same minimum deflection. Note that the first term of the infinite series for Hencky's solution is a 2nd order polynomial, hence the usage of a circular paraboloid as an approximation for the bulge shape.

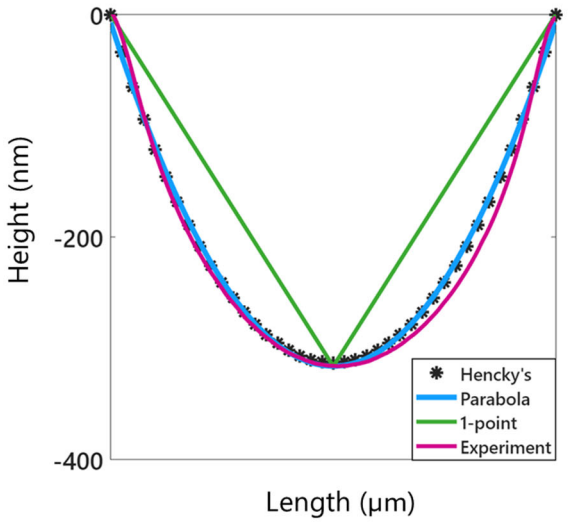

Figure S1. Approximations of a gas-filled bulge (pink) with Hencky's solution (black), a second-order polynomial (blue), and the one-point model (green).

Correlations of Different Physical Length Scales with MSD

In addition to the analysis in *Figure 2*, we analyzed the correlation between the MSD of all bulges and their initial heights (*Figure S2 i*), initial pressure differences across the well (*Figure S2 ii*), and initial bulge surface areas (*Figure S2 iii*). To calculate the pressure difference across the well, we started with the known initial heights information and used Hencky's solution in combination with reported elastic moduli and Poisson's ratios[3–5] to obtain the pressure difference.

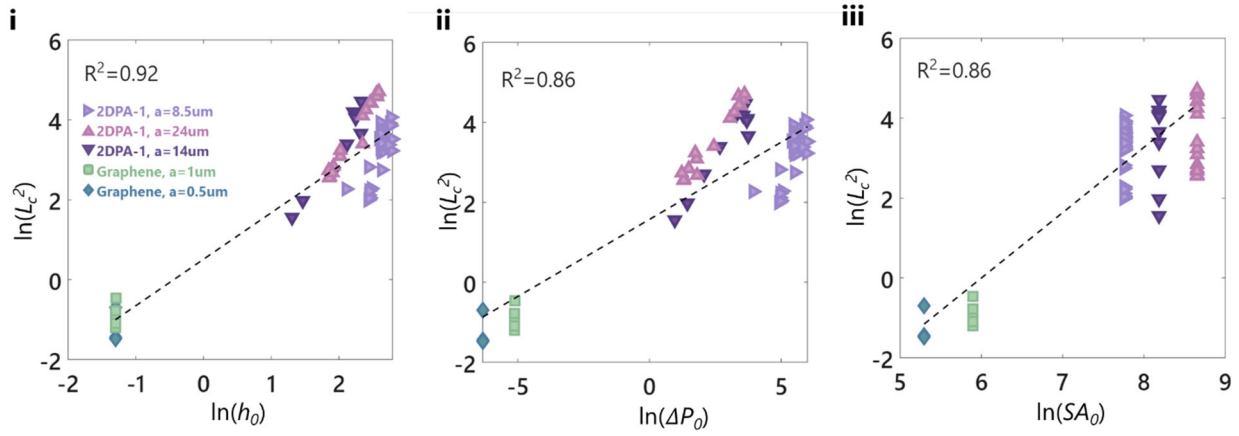

Figure S2. Comparisons of $\ln(L_c^2)$, for graphene bulges (green square: a=1μm; blue diamond: a=0.5μm) and 2DPA-1 bulges (left pointing triangle: a=8.5μm; upwards pointing triangle: a=24μm; downwards pointing triangle: a=14μm) with (i) logarithm of initial height, h_0; (ii) logarithm of calculated initial pressure difference, ΔP_0; and (iii) logarithm of initial bulge surface area, SA_0.

Impact of Ambient Fluctuations on Gas Volume and Bulge Height

Over a 5-month period, we measured with a temperature sensor (SensorPush HT1 Smart Sensor) that the temperature fluctuates in one lab room between 66.5 and 71.5°F, or up to approximately a difference of 3°C. We calculate the effect of this temperature calculation on our samples by estimating the thermal expansion of our silicon substrates. The linear expansion equation, which estimates how much a material expands/contracts, ΔL, for a given temperature change, ΔT, is:

$$\Delta L = \alpha L_0 \Delta T \quad \text{Equation S3}$$

where α is the coefficient of thermal expansion (2.6 1/°C for silicon) and L_0 is the initial length. Our substrates are on the order of 1 cm by 1 cm in area. Thus, using the above expression, we can calculate that for a 3°C change in temperature, 1 cm of silicon changes by 78 nm. On the scale of a well diameter, which is at most 24um, this would be a change in length of 0.19nm. In terms of the effect on the bulge volume, this would thus be negligible.

We can also calculate the effect of ambient fluctuations on gas expansion/contraction and thus on a bulge's height by combining Hencky's solution with the ideal gas law, assuming the bulges are impermeable. This results in *Equation 8* from the main text. We find that for bulges starting at 100 nm, subjected to a 3°C temperature fluctuation, the gas inside will change the deflection in the following way:

Material	**Well Type**	**Starting δ (nm)**	**Change in δ (nm)**
2DPA-1	Substrate II	100	5
2DPA-1	Substrate I, a=14um	100	37
2DPA-1	Substrate I, a=24um	100	141
Graphene	A=0.5um	100	0.27
Graphene	A=1um	100	0.27

These predicted changes are of the same order of magnitude as the noted experimental fluctuations.

We notice that experimental fluctuations appear correlated between multiple bulges. We analyzed how the height fluctuates for all 25 bulges shown in *Figure 2A*. We calculated the difference in δ between measurements, $\Delta\delta$, for all bulges and compared the $\Delta\delta$ of bulges that are on the same silicon wafer substrate (as they were all measured on the same day; this is at least 11 time points and at most 24 depending on the sample). The R^2 values of all comparisons are compiled in *Figure S3a*. Of the 59 comparisons, more than 50% have $R^2>0.8$ and almost 75% of comparisons have $R^2>0.7$. Moreover, we compared the $\Delta\delta$ of these bulges across samples (only comparing data that was obtained on the same day, for a total of 6 time points). Again, more than 50% of the comparisons have $R^2>0.8$ (*Figure S3b*). Altogether, the strong correlations between $\Delta\delta$ of bulges on the same sample and between different samples imply that parameters related to daily conditions, such as atmospheric temperature and pressure, cause the δ fluctuations.

To understand if the model predicts the fluctuations seen experimentally, we measured the δ of a single bulge shown in *Figure 2A* (d=12.8 nm, a=24um) over 4 days and recorded the T and p_0 of the measuring room for each day. Then, we calculated using *Equation 8* the predicted δ of the bulge, assuming no permeation (*Figures S3c and S3d*). We find that both the magnitude of the change and the direction of the height change are not accurately captured with this model. We hypothesize that there could be a delayed impact of the atmospheric conditions on the bulges, as there is a strong correlation between the height fluctuations, yet these cannot be captured accurately with *Equation 8*.

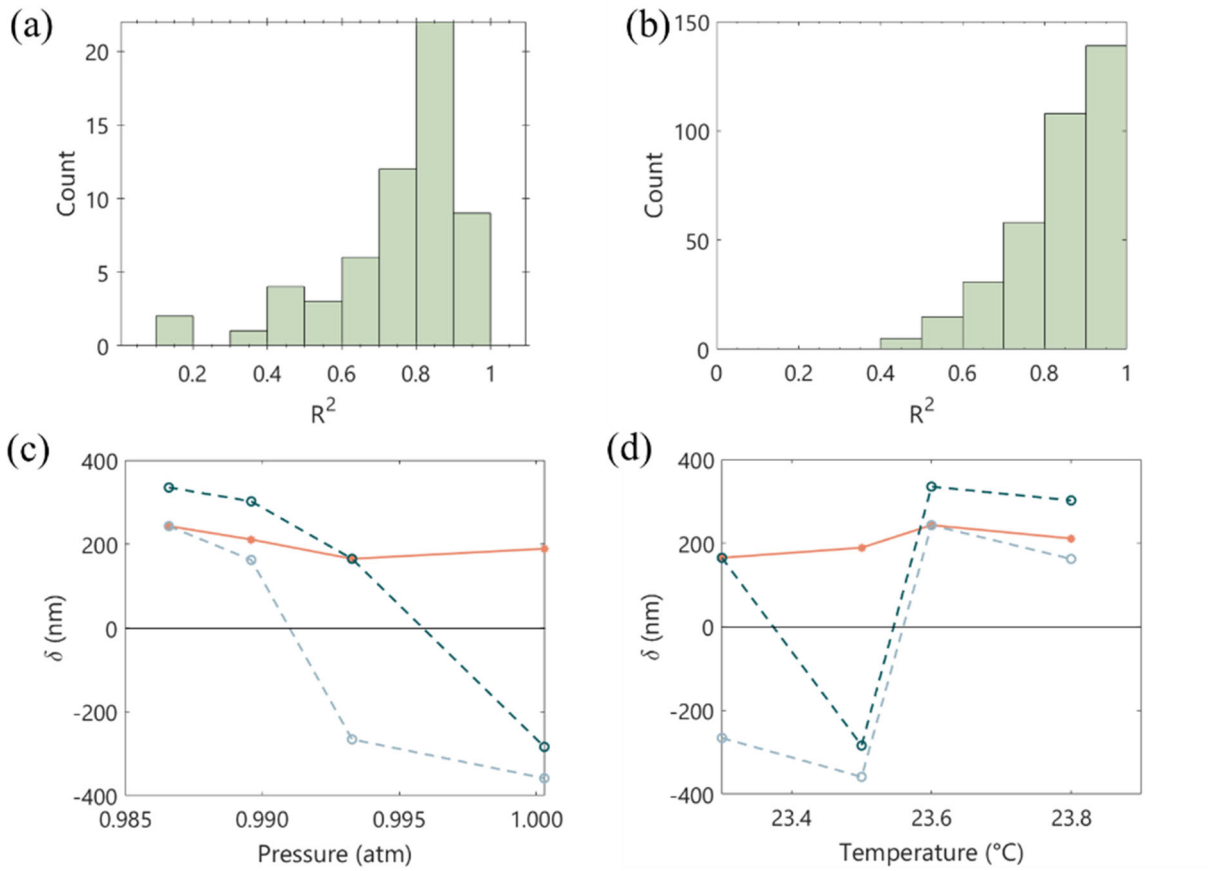

Figure S3. Analysis of data variation. (a) R^2 values for correlations between the height fluctuations of bulges on the same samples. Comparisons are only between measurements taken on the same day. (b) R^2 values for correlations between height fluctuations of bulges on different samples. Comparisons are only between measurements taken on the same day. (c,d) Experimental data of one bulge (red) compared to theoretical bulge heights (blue) versus p_0 (c) and T (d), assuming that n is constant between measurements. n is calculated using the highest δ (light blue) and the lowest δ (dark blue) value to show the range of predicted δ.

Diameter Variation for Bulges used in MSD Analysis

The bulges monitored in Figure 2 do not exhibit significant or correlative changes in their diameters throughout the experiment. We include the calculated diameters from AFM data sets for all of the data points for the 24μm and 14μm average-diameter bulges.

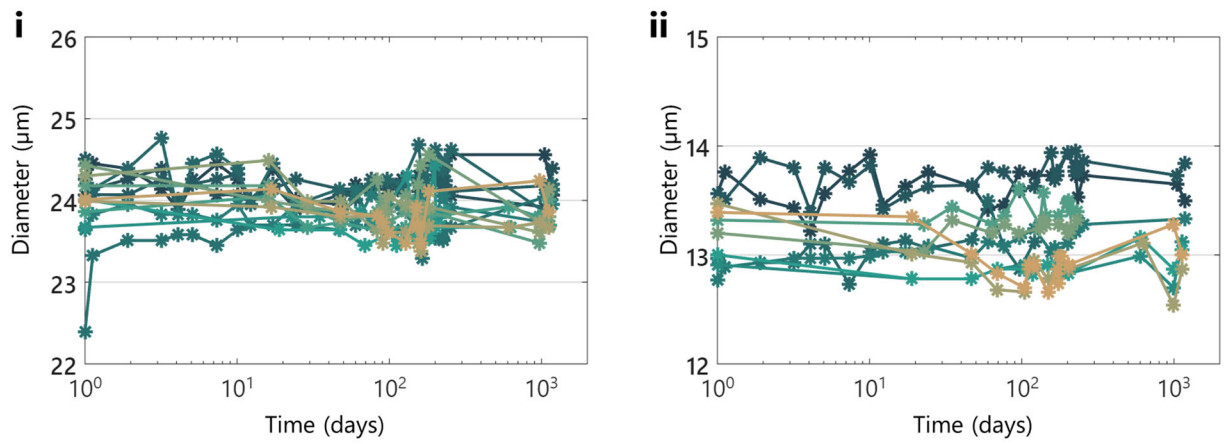

Figure S4. Analysis of the bulge diameters used for the MSD analysis. A) Changes in the 24µm average-diameter bulges, B) Changes in the 14µm average-diameter bulges.

Validation of Bulge Stability via Puncturing

The persistence of a bulge as an indication of impermeability can be validated through the introduction of a controlled puncture; there are noted instances of defects being introduced to single layer graphene samples with laser-induced heating and AFM tips,[6,7] resulting in a measurable permeance. We sought to puncture a series of positively-deflected N_2-filled 2DPA-1 bulges using an AFM tip (AC 240) to validate that the observed, persistent upwards-deflection is indeed reflective of N_2 impermeability.

We found two different types of behaviors once the bulges were punctured with an AFM tip; the bulges that resort to their un-filled states (*Figure S4 A and B*) and bulges that do not (*Figure S4 C*). We attribute this difference in behavior to the interaction of the tip with the bulge. Within the bulge test system outside of an AFM, the sole force impacting the shape of the bulge is that of the pressure difference across it, which is what yields the often used Hencky's solution.[1] A positively-deflected bulge has a higher pressure of gas on its interior than exterior. When an AFM tip is introduced, there is a complex interplay of both attractive and repulsive forces between the AFM tip and sample which can be affected by factors such as tip geometry, tip material, and atmospheric humidity. In cases where we applied minimal contact (*Figure S4 A and B*), the AFM tip minimally interacted with the bulge in terms of region (*Figure S4 A*) or time (*Figure S4 B*), and thus as the gas leaked out of the bulge, the only force supporting its upwards deflection was removed. In cases where we applied more contact (*Figure S4 C*), we hypothesize that the AFM tip exerted an upwards force on the bulge as it was being removed, which then left the bulge in a positively-deflected state. Thus, puncturing the bulges can be used to validate that the bulges were indeed containing gas throughout the measurement, but only if the puncture is done with minimal AFM tip contact.

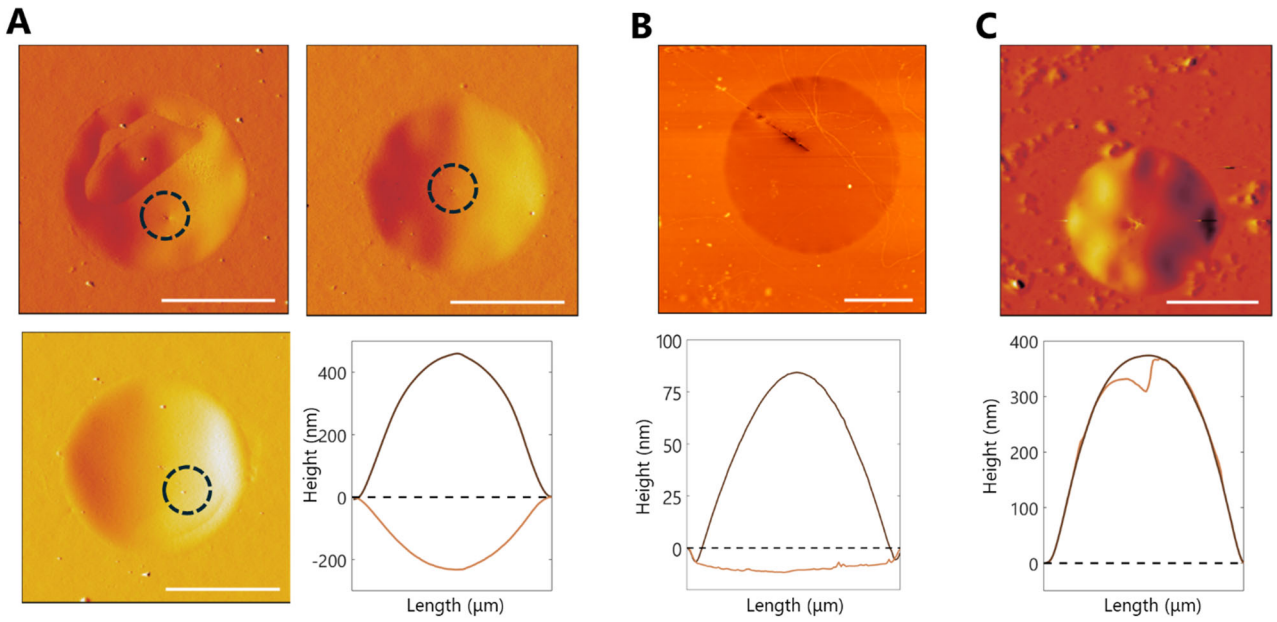

Figure S5.
Bulges punctured using contact mode of the Cypher S AFM. Amplitude graphs are shown, as these most clearly show the punctured regions; scale bar indicates 5µm. Bulges that are punctured with minimal AFM tip contact based on space (A) or time (B) and bulges that are punctured with non-minimal contact (C) exhibit different deflation behavior. Pre-punctured 2D profiles are shown in dark brown while post-puncture profiles are shown in orange. Bulges in A and C are on Substrate II and bulge in B is on Substrate I.

(1) H. Hencky. Uber den Spannungszustand in kreisrunden Platten mit verschwindender Biegungssteifigkeit. *Z. Math. Phys.* **1915**, *63*, 311–317.
(2) Fichter, W. B. Some Solutions for the Large Deflections of Uniformly Loaded Circular Membranes.
(3) Sun, P. Z.; Yang, Q.; Kuang, W. J.; Stebunov, Y. V.; Xiong, W. Q.; Yu, J.; Nair, R. R.; Katsnelson, M. I.; Yuan, S. J.; Grigorieva, I. V.; Lozada-Hidalgo, M.; Wang, F. C.; Geim, A. K. Limits on Gas Impermeability of Graphene. *Nature* **2020**, *579* (7798), 229–232. https://doi.org/10.1038/s41586-020-2070-x.
(4) Koenig, S. P.; Boddeti, N. G.; Dunn, M. L.; Bunch, J. S. Ultrastrong Adhesion of Graphene Membranes. *Nat. Nanotechnol.* **2011**, *6* (9), 543–546. https://doi.org/10.1038/nnano.2011.123.
(5) Zeng, Y.; Gordiichuk, P.; Ichihara, T.; Zhang, G.; Sandoz-Rosado, E.; Wetzel, E. D.; Tresback, J.; Yang, J.; Kozawa, D.; Yang, Z.; Kuehne, M.; Quien, M.; Yuan, Z.; Gong, X.; He, G.; Lundberg, D. J.; Liu, P.; Liu, A. T.; Yang, J. F.; Kulik, H. J.; Strano, M. S. Irreversible Synthesis of an Ultrastrong Two-Dimensional Polymeric Material. *Nature* **2022**, *602* (7895), 91–95. https://doi.org/10.1038/s41586-021-04296-3.
(6) Drahushuk, L. W.; Wang, L.; Koenig, S. P.; Bunch, J. S.; Strano, M. S. Analysis of Time-Varying, Stochastic Gas Transport through Graphene Membranes. *ACS Nano* **2016**, *10* (1), 786–795. https://doi.org/10.1021/acsnano.5b05870.
(7) Wang, L.; Drahushuk, L. W.; Cantley, L.; Koenig, S. P.; Liu, X.; Pellegrino, J.; Strano, M. S.; Scott Bunch, J. Molecular Valves for Controlling Gas Phase Transport Made from Discrete Ångström-Sized Pores in Graphene. *Nat. Nanotechnol.* **2015**, *10* (9), 785–790. https://doi.org/10.1038/nnano.2015.158.